Zfp281 mediates Nanog autorepression through recruitment of the NuRD complex and inhibits somatic cell reprogramming

Miguel Fidalgo[a], Francesco Faiola[a], Carlos-Filipe Pereira[a], Junjun Ding[a], Arven Saunders[a,b], Julian Gingold[a,b], Christoph Schaniel[a], Ihor R. Lemischka[a], José C. R. Silva[c], and Jianlong Wang[a,b,1]

[a]Department of Developmental and Regenerative Biology, Black Family Stem Cell Institute, and [b]The Graduate School of Biological Sciences, Mount Sinai School of Medicine, New York, NY 10029; and [c]Wellcome Trust–MRC Stem Cell Institute and Department of Biochemistry, University of Cambridge, Cambridge CB2 1QR, United Kingdom

Edited* by Rudolf Jaenisch, Whitehead Institute for Biomedical Research, Cambridge, MA, and approved August 22, 2012 (received for review May 22, 2012)

The homeodomain transcription factor Nanog plays an important role in embryonic stem cell (ESC) self-renewal and is essential for acquiring ground-state pluripotency during reprogramming. Understanding how Nanog is transcriptionally regulated is important for further dissecting mechanisms of ESC pluripotency and somatic cell reprogramming. Here, we report that Nanog is subjected to a negative autoregulatory mechanism, i.e., autorepression, in ESCs, and that such autorepression requires the coordinated action of the Nanog partner and transcriptional repressor Zfp281. Mechanistically, Zfp281 recruits the NuRD repressor complex onto the *Nanog* locus and maintains its integrity to mediate Nanog autorepression and, functionally, Zfp281-mediated Nanog autorepression presents a roadblock to efficient somatic cell reprogramming. Our results identify a unique transcriptional regulatory mode of Nanog gene expression and shed light into the mechanistic understanding of Nanog function in pluripotency and reprogramming.

iPSC | Nanog autoregulation

An understanding of the molecular underpinnings of stem cell pluripotency and somatic cell reprogramming is a prerequisite for therapeutic application of embryonic stem cells (ESCs) and induced pluripotent stem cells (iPSCs). Initial efforts in dissecting transcriptional (1) and protein interaction (2–4) networks operative in ESCs form a foundation for such mechanistic studies. The common view of the Oct4-Sox2-Nanog network suggests that these core factors activate their own expression and each other's expression to form a positive feedback circuit (5). Although it is well recognized that a negative feedback mechanism must exist to fine-tune this core network and allow for optimal expression of these dosage-sensitive transcription factors, it remains to be determined how these core factors execute a "self-control" regulatory mechanism to prevent excessive expression in maintaining the ESC state.

Enforced expression of Nanog relieves ESCs from their leukemia inhibitory factor (LIF) requirement (6), promotes transfer of pluripotency after cell fusion (7), and ensures direct reprogramming of somatic cells to the pluripotent ground state (8). How Nanog is transcriptionally regulated and participates in the transcriptional machinery to control pluripotency and reprogramming is still poorly understood. Several modes of *Nanog* gene regulation have been published. First, during the early differentiation process of ESCs *Nanog* (and *Oct4*) is subjected to epigenetic regulation at its enhancer/promoter region by DNA methyltransferases (9) and histone methyltransferases (10). Second, studies have documented direct transcriptional regulation of *Nanog* by both positive and negative regulators (11). Third, the Nanog interactome contains many factors whose genes are also downstream targets of themselves, thus forming autoregulatory loops in the pluripotency network (3, 12). Nanog is known to regulate its own expression by positive feedback in ESCs (i.e., autoactivation) (13), which in one case was shown to be mediated by the Nanog partner and transcriptional regulator Sall4 (14). However, the fine-tuning of Nanog levels is necessary for balancing self-renewal and pluripotency of ESCs as too much Nanog favors self-renewal and impedes the execution of pluripotency under proper differentiation cues (6). Little is known about whether negative autoregulatory feedback, i.e., autorepression, exists in ESCs to control *Nanog* expression and how such autorepression relates to its function in pluripotency and reprogramming.

In this study, we provide molecular and biochemical data uncovering Nanog autorepression as a unique transcriptional regulatory mode of *Nanog* expression in ESCs. We establish Zfp281 as an important *Nanog* regulator and cofactor that mediates Nanog autorepression through recruitment and maintenance of the NuRD repressor complex on the *Nanog* locus and that restricts *Nanog* reactivation during somatic cell reprogramming.

Results

Nanog Is Subjected to Autorepression in ESCs. To test whether Nanog autorepression exists in ESCs, we performed both Nanog overexpression and knockdown studies in NG4 transgenic ESCs expressing the enhanced green fluorescent protein (GFP) reporter gene under the control of the endogenous *Nanog* promoter (P_{Nanog}) (Fig. 1*A*, *Left*) (15). First, we introduced a doxycycline (Dox)-inducible *Nanog* transgene bearing a Flag-biotin dual tag (FLbio) and established stable clones by puromycin selection (Fig. 1*A*, *Right*). We found that induced expression of ^{FLbio}*Nanog* upon Dox treatment (Fig. 1*B*, *Left* and *C*) resulted in down-regulation of both endogenous *Nanog* (^{Endo}*Nanog*) transcripts (Fig. 1*B*, *Right*) and protein (Fig. 1*C*) and *Nanog*-GFP reporter activity (Fig. 1*D*) in a dose-dependent manner. We then asked whether knockdown of ^{Endo}*Nanog* expression would enhance transgenic *Nanog*-GFP reporter expression. We infected NG4 cells with lentiviruses expressing a constitutive shRNA against the 3′-UTR of *Nanog* (shNanog) (Fig. 1*A* and Table S1). *Nanog*-GFP reporter activity was measured over a 5-d period by flow cytometry. We confirmed efficient knockdown of *Nanog* by RT-quantitative PCR (qPCR) (Fig. 1*E*), and more importantly, we found that *Nanog*-GFP reporter activity was up-regulated over the time course (Fig. 1*F*). In contrast, the control shRNAs (shEmpty and shLuci) affected neither ^{Endo}*Nanog* expression levels (Fig. 1*E*) nor *Nanog*-GFP reporter activity (Fig. 1*F*). These results support the existence of Nanog autorepression as a regulatory mode of Nanog expression in ESCs.

To confirm that Nanog autorepression is a general phenomenon in ESCs, we further examined the effects of enforced *Nanog* expression on ^{Endo}*Nanog* levels in a previously published episomal overexpression system in E14T ESCs (6) (Fig. S1*A*). Consistent with the published study, we confirmed enhanced ESC self-renewal (Fig. S1*B*) and an overall increase in Nanog expression at both total transcript (Fig. S1*C*) and protein levels

Author contributions: M.F. and J.W. designed research; M.F., F.F., C.-F.P., J.D., A.S., J.G., and J.W. performed research; C.S., I.R.L., and J.C.R.S. contributed new reagents/analytic tools; M.F., F.F., C.-F.P., J.G., and J.W. analyzed data; and M.F. and J.W. wrote the paper.

The authors declare no conflict of interest.

*This Direct Submission article had a prearranged editor.

[1]To whom correspondence should be addressed. E-mail: jianlong.wang@mssm.edu.

This article contains supporting information online at www.pnas.org/lookup/suppl/doi:10.1073/pnas.1208533109/-/DCSupplemental.

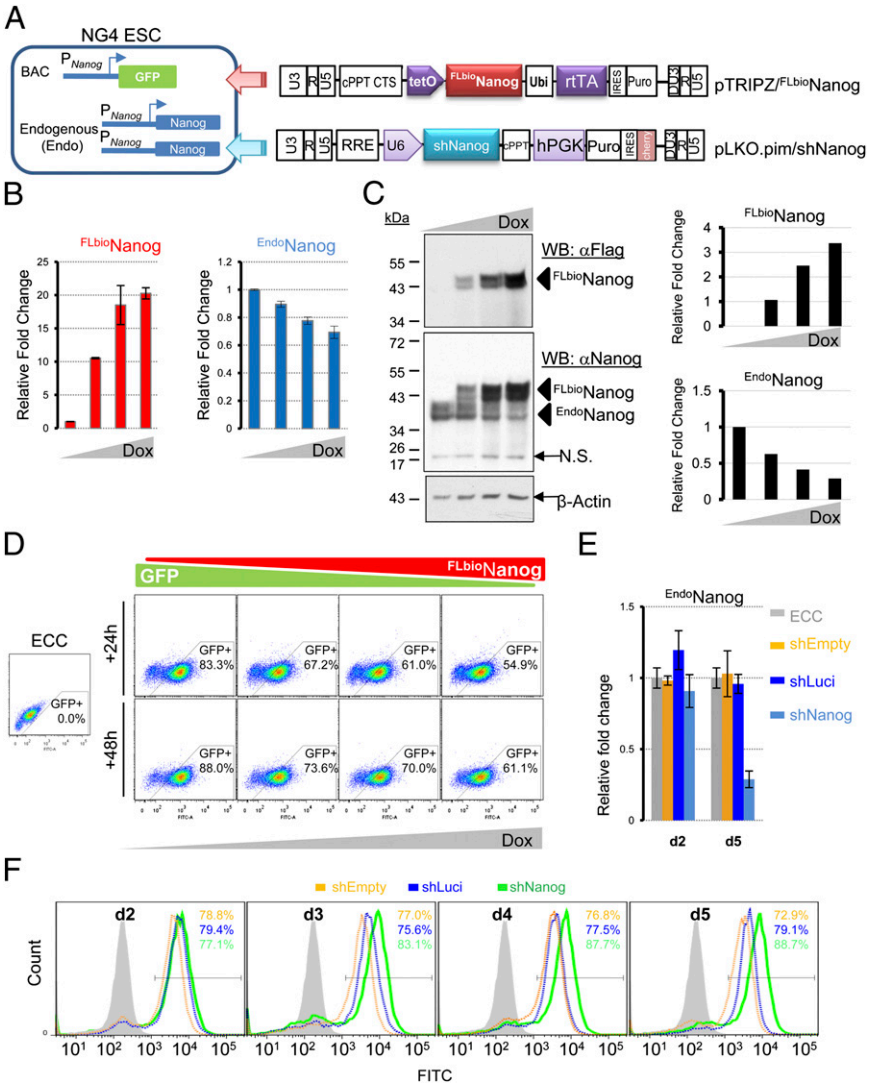

Fig. 1. Nanog autorepression in ESCs. (*A*) The strategy for inducible ^{FLbio}*Nanog* expression or constitutive *Nanog* knockdown by shRNA (shNanog) in NG4 ESCs. (*B*) RT-qPCR analyses of ectopic (^{FLbio}*Nanog*) and endogenous (^{Endo}*Nanog*) expression of *Nanog* upon Dox (0, 0.625, 1.25, or 2.5 μg/mL) treatment. (*C*) Western blotting (WB) analyses of ^{FLbio}*Nanog* and ^{Endo}*Nanog* expression upon Dox treatment. Western gel images are shown on *Left*, and quantitation of the western signals is on *Right*. N.S., nonspecific signal. (*D*) Flow cytometry analyses of *Nanog*-GFP reporter activity upon Dox treatment for 24 and 48 h. The parental ESC line of NG4 cells (ECC) was used as a GFP negative control. (*E*) RT-qPCR analyses of ^{Endo}*Nanog* expression upon Nanog knockdown (shNanog) in NG4 ESCs. ECC line and stable NG4 transgenic lines infected with pLKO lentiviruses expressing no shRNA (shEmpty) or shRNA against luciferase (shLuci) were used as controls. (*F*) Flow cytometry analyses of *Nanog*-GFP reporter activity upon shRNA-mediated knockdown as indicated.

(Fig. S1*D*). More importantly, we found that ectopic Nanog expression led to down-regulation of ^{Endo}*Nanog* transcript levels (Fig. S1*E*), supporting Nanog autorepression in ESCs. Together, these results establish a mode of *Nanog* transcriptional regulation, i.e., Nanog autorepression, in ESCs.

Zfp281 Is Required for Nanog Autorepression via Its Association with the NuRD Repressor Complex in ESCs. To gain insight into the molecular mechanism of Nanog autorepression in ESCs, we focused on the Krüppel-like zinc finger transcription factor Zfp281. We reported it to be a close partner of Nanog (3) and later demonstrated it to be a transcriptional repressor to restrict *Nanog* expression in maintaining ESC pluripotency (16). In this study, we evaluated how knockdown of Zfp281 might affect ^{Endo}*Nanog* and *Nanog*-GFP reporter expression in NG4 cells (Fig. 2*A*). Using a Dox-inducible Zfp281 shRNA (Table S1), we demonstrated that down-regulation of *Zfp281* upon Dox induction (Fig. 2*C*, gray bars) led to an increase in both transgenic *Nanog*-GFP reporter activity (Fig. 2*B*) and ^{Endo}*Nanog* transcript levels (Fig. 2*C*, blue bars). These results confirm that Zfp281 functions as a transcriptional repressor for *Nanog* expression in ESCs and suggest that Zfp281 may play a role in Nanog autorepression. To test whether Zfp281 is necessary for Nanog autorepression, we infected both *Zfp281* wild-type ($Zfp281^{+/+}$) and null ($Zfp281^{-/-}$) ESCs (16) with lentiviruses expressing a Dox-inducible ^{FLbio}*Nanog* transgene (Fig. 2*D*) and examined ^{Endo}*Nanog* expression upon Dox treatment. We confirmed Dox-dependent up-regulation of ^{FLbio}*Nanog* expression in both $Zfp281^{+/+}$ and $Zfp281^{-/-}$ ESCs (Fig. 2 *E* and *F*, *Left*). Importantly, although we observed (as expected) down-regulation of ^{Endo}*Nanog* transcript levels in $Zfp281^{+/+}$ ESCs (Fig. 2*E*, *Right*), we found that inducible ^{FLbio}*Nanog* overexpression in $Zfp281^{-/-}$ cells failed to repress *Nanog* promoter activity. Intriguingly, ^{Endo}*Nanog* expression increased in a dose-dependent manner (Fig. 2*F*, *Right*). These results demonstrate that Zfp281 is required for Nanog autorepression, and that Nanog is able to activate its own promoter, either directly or indirectly, in the absence of Zfp281 (see more in *Discussion*).

To further explore the molecular mechanism by which Zfp281 mediates Nanog autorepression, we tested whether Zfp281 may assist Nanog in recruiting certain corepressor complexes into the *Nanog* promoter/enhancer region for transcriptional repression. We performed affinity purification of Zfp281 protein complexes in wild-type ESCs by using an anti-Zfp281 antibody (Fig. S2) and identified Zfp281-associated proteins by mass spectrometry. Our results indicate a preferential association of Zfp281 with all the major NuRD components in ESCs (Fig. 2*G*). We confirmed the endogenous association of Zfp281 with Nanog and with the NuRD components Mta1/2, Hdac2, and Chd4 (Mi-2β) by performing immunoprecipitation (IP) with antibodies against Nanog, Zfp281, and NuRD proteins in both $Zfp281^{+/+}$ and $Zfp281^{-/-}$ ESCs (Fig. 2*H*). Interestingly, we found that, although endogenous association of the core NuRD protein Chd4 with Mta1/2 and Hdac2 is readily detected in wild-type ESCs, it is greatly diminished

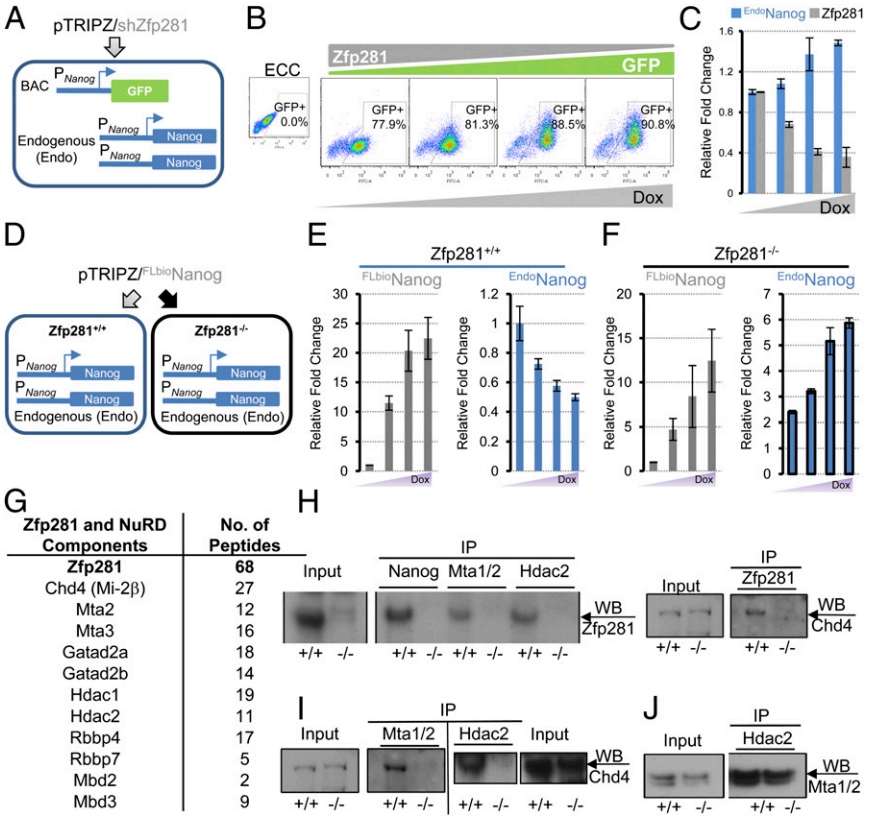

Zfp281 and NuRD Components	No. of Peptides
Zfp281	**68**
Chd4 (Mi-2β)	27
Mta2	12
Mta3	16
Gatad2a	18
Gatad2b	14
Hdac1	19
Hdac2	11
Rbbp4	17
Rbbp7	5
Mbd2	2
Mbd3	9

Fig. 2. Zfp281 is required for Nanog autorepression and the integrity of the NuRD repressor complex in ESCs. (*A*) The strategy for inducible knockdown of Zfp281 in NG4 cells. (*B*) Flow cytometry analyses of *Nanog*-GFP reporter activity upon shRNA-mediated knockdown of Zfp281. *Nanog*-GFP was analyzed 3d after puromycin selection and Dox treatment. (*C*) RT-qPCR analyses of ^{Endo}*Nanog* and *Zfp281* expression in the samples described in *B*. (*D*) The strategy for inducible ^{FLbio}*Nanog* expression in both *Zfp281*$^{+/+}$ and *Zfp281*$^{-/-}$ ESCs. (*E* and *F*) RT-qPCR analyses of ^{FLbio}*Nanog* and ^{Endo}*Nanog* expression upon Dox treatment in *Zfp281*$^{+/+}$ (*E*) and *Zfp281*$^{-/-}$ (*F*) ESCs. (*G*) Zfp281 is associated with the NuRD repressor complex in ESCs. Total peptide numbers identified by mass spectrometry are listed. (*H*) Confirmation of endogenous association of Zfp281 with Nanog and the NuRD proteins by immunoprecipitation (IP) and WB analyses in *Zfp281*$^{+/+}$ and *Zfp281*$^{-/-}$ ESCs. (*I*) Zfp281 is required for the integrity of the NuRD repressor complex. (*J*) Interaction between Mta1/2 and Hdac2 is not affected by Zfp281 depletion.

in the absence of Zfp281 (Fig. 2*I, Left*). In contrast, the interactions between other "peripheral" NuRD proteins (e.g., Hdac2 and Mta1/2) are maintained regardless of *Zfp281* expression (Fig. 2*J*), suggesting that Zfp281 might be an important factor to maintain the physical and functional integrity of the NuRD complex in ESCs. Taken together, our data demonstrate a critical role of Zfp281 in mediating Nanog autorepression through its interaction with the NuRD repressor complex.

Zfp281 Mediates Nanog Autorepression by Directly Recruiting the NuRD Repressor Complex to the *Nanog* Locus. The association of both Nanog (3, 17) and Zfp281 (Fig. 2 *G* and *H*) with the NuRD repressor complex prompted us to investigate the mechanistic action of the NuRD complex in Nanog autorepression. First, we used chromatin immunoprecipitation (ChIP) coupled with qPCR (ChIP-qPCR) to analyze whether Zfp281 is required for recruitment of NuRD proteins to the *Nanog* regulatory regions (Fig. 3*A*). Consistent with a previous report (17) and our coimmunoprecipitation (co-IP) data (Fig. 2*H*), we confirmed that Nanog, Mta1/2, and Hdac2 occupy the *Nanog* enhancer region (sites B′ and B″) and, to a lesser extent, the promoter region (site C) (Fig. 3*B*, black bars), but not a remote control region (Fig. 3*A*, A). More importantly, we found that binding of Nanog, Mta1/2, and Hdac2 to these regulatory regions (B′, B″, and C) is drastically diminished upon Zfp281 depletion (Fig. 3*B*, gray bars), an effect that is not due to down-regulation of protein levels (Fig. 3*C*).

Next, we examined the occupancy of Nanog, Zfp281, and NuRD proteins on the *Nanog* enhancer upon inducible *Nanog* overexpression in NG4 ESCs (Fig. 3*D*). ChIP-qPCR analysis not only confirmed binding of endogenous Nanog, Zfp281, and Mta1/2 to the *Nanog* enhancer (site B′) in these cells (Fig. 3*E*, black bars), but also revealed enhanced binding of these factors upon Dox-induced ^{FLbio}*Nanog* expression (Fig. 3*E*, gray bars). These data support the notion that Nanog autorepression is likely mediated by Zfp281 and its associated NuRD repressor complex. To address whether Nanog autorepression depends on the NuRD repressor complex, we introduced lentiviral shRNAs against NuRD complex proteins (Chd4, Gatad2b, Mta2, and Mta3) into the Dox-inducible ^{FLbio}*Nanog* transgenic line as shown in Fig. 3*D* (Fig. 3*F*). The expression of these shRNAs in NG4 ESCs caused a reduction of corresponding gene expression by 80–90% compared with the control knockdown (shEmpty) (Fig. 3*G*). As expected, control cells without virus infection or with infection of empty shRNA virus (shEmpty) exhibit Nanog autorepression upon inducible ^{FLbio}*Nanog* expression (+Dox), as measured by flow cytometry of *Nanog*-GFP reporter activity (Fig. 3*H*, compare the black bars with the gray bars in the first two columns). Importantly, down-regulation of the NuRD proteins Chd4, Gatad2b, Mta2, and Mta3 by shRNAs attenuates or abrogates such autorepression (Fig. 3*H*, bars in the last four columns), which indicates that the NuRD complex is necessary for Zfp281-mediated Nanog autorepression. Together, these data demonstrate that Zfp281 mediates Nanog autorepression through recruitment of the NuRD repressor complex onto the *Nanog* locus in ESCs.

Zfp281 Restricts *Nanog* Reactivation and Inhibits Somatic Cell Reprogramming. Because Nanog is essential for achieving ground-state pluripotency of iPSCs, we examined whether Zfp281 may play a role in somatic cell reprogramming by influencing *Nanog* expression. We used mouse embryonic fibroblasts (MEFs) harboring an *Oct4* promoter-driven GFP reporter transgene (*Oct4*-GFP) for iPSC generation by following the standard iPSC generation protocol (18) with modifications (Fig. 4*A*). First, we evaluated relative *Zfp281* and *Nanog* gene expression during the reprogramming process. We found that both *Zfp281* and *Nanog* are up-regulated during reprogramming, and up-regulation of *Zfp281* precedes the reactivation of *Nanog* gene expression (Fig. 4*B*). This result suggests that Zfp281 may restrict *Nanog* reactivation during the reprogramming process and likely also plays a similar role in fine-tuning Nanog levels in iPSCs as that in ESCs (16) to maintain pluripotency.

We then tested the effects of Zfp281 knockdown (KD) on *Nanog* reactivation during iPSC generation (Fig. 4*A*). We coinfected *Oct4*-GFP MEFs with lentiviruses constitutively expressing the reprogramming factor mixture (Oct4, Sox2, Klf4, and c-Myc; OSKM) and short hairpin RNAs (shRNAs) against

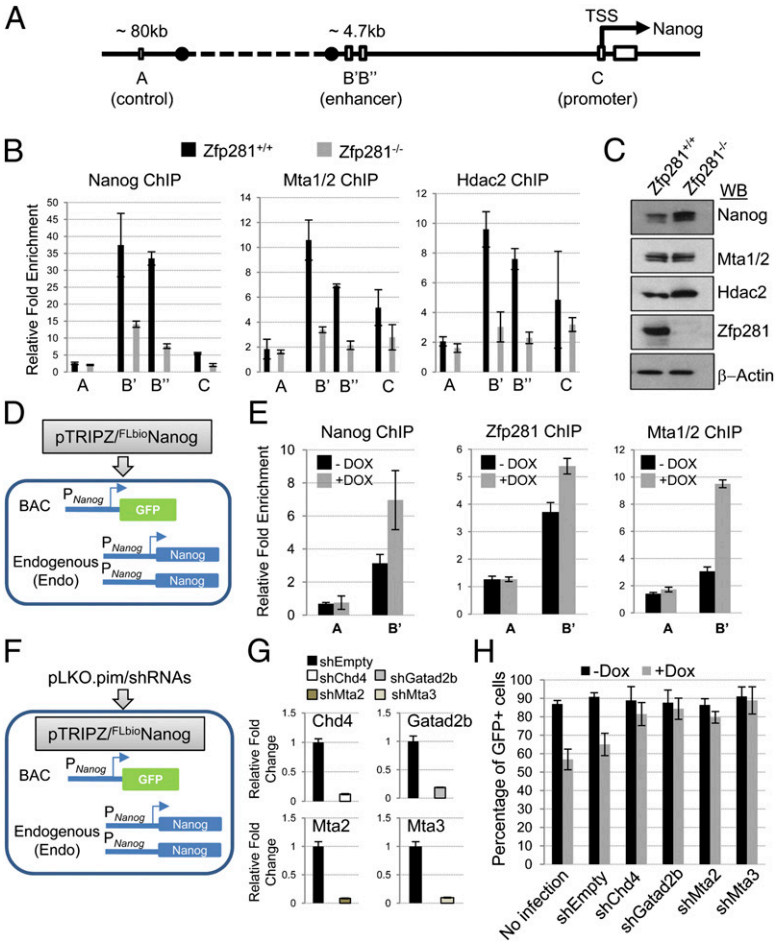

Fig. 3. Requirement of the NuRD repressor complex for Nanog autorepression. (*A*) Illustration of the upstream regulatory regions of the *Nanog* gene. The amplicons corresponding to a control region, the enhancer, and the promoter are indicated as A, B′/B′′, and C, respectively. TSS, transcription start site. (*B*) Relative enrichment of Nanog, Mta1/2, and Hdac2 in the genomic loci of *Nanog* in *Zfp281*$^{+/+}$ and *Zfp281*$^{-/-}$ ESCs. (*C*) WB analyses of Nanog, Mta1/2, Hdac2, and Zfp281 in *Zfp281*$^{+/+}$ and *Zfp281*$^{-/-}$ ESCs. (*D* and *E*) A Dox-inducible Nanog expression cell system (*D*) indicates that ectopic *Nanog* expression by Dox promotes Nanog, Zfp281, and Mta1/2 binding to the *Nanog* enhancer (*E*). ESCs without (–) or with (+) Dox (1.5 μg/mL) treatment for 48 h were harvested for ChIP-qPCR analyses. (*F*) The strategy for knockdown of NuRD proteins in NG4 ESCs that express inducible ^{FLbio}*Nanog*. (*G*) Efficient knockdown of NuRD proteins in NG4 ESCs analyzed by RT-qPCR. Expression levels of individual genes upon knockdown were normalized to the control knockdown (shEmpty). (*H*) Knockdown of NuRD protein expression reduces or abrogates Nanog autorepression in ESCs. The *Nanog*–GFP-positive cell population in uninfected samples (no infection) or the GFP/mCherry–double-positive cell population (shRNA-transduced cells) were measured after treatment with or without Dox (2 μg/mL) for 24 h.

Zfp281. We used three independent shRNAs that reduced *Zfp281* expression by 60–80% relative to the control scramble shRNA (shSCR) (Fig. S3*A*). Consistent with its function in mediating Nanog autorepression, knockdown of Zfp281 resulted in up-regulation of *Nanog* during the reprogramming process, in particular, during the late stages (d17 and thereafter) of reprogramming (Fig. 4*C*). We confirmed that there is no significant change in MEF growth rates between scramble (shSCR) and Zfp281 shRNAs (Fig. S3*B*). Importantly, we found that, although loss of Zfp281 minimally affects the total number of AP-positive colonies (Fig. 4*D* and Fig. S3*C*), it markedly reduces the number of *Oct4*–GFP-negative, partially reprogrammed colonies (Fig. 4*E*, yellow bars/pies) and increases the percentage of overall *Oct4*–GFP-positive, fully pluripotent iPSC colonies (Fig. 4*E*, green bars/pies and Fig. S3*D*). Flow cytometry analysis of *Oct4*-GFP reporter activity further confirmed an increase in the percentage of GFP-positive cells when Zfp281 is down-regulated during reprogramming (Fig. S3*E*).

Together, our data demonstrate that the transcriptional repressor Zfp281 restricts *Nanog* reactivation during the reprogramming process and, thus, functions as a molecular barrier to the transition of intermediate cells or so-called "pre-iPSCs" (19) into ground-state, pluripotent iPSCs.

Zfp281 Depletion Promotes the PreiPSC to iPSC Transition Through *Nanog* Regulation. To directly address whether Zfp281 depletion can promote the preiPSC to iPSC transition as suggested above, we used a published reprogramming system that allows direct investigation of the preiPSC to iPSC transition (19). In this system, preiPSCs generated from Oct4, Klf4, and c-Myc (OKM)-transduced wild-type neural stem cells harboring an *Oct4*-GFP reporter transgene are maintained in normal serum/LIF culture. Only a minority of these preiPSCs will become iPSCs after switching to the 2i/LIF condition, and the reprogramming efficiency can be greatly enhanced if exogenous Nanog is provided (20). We asked whether down-regulation of Zfp281 could replace the requirement for exogenous Nanog to promote the *Nanog*$^{+/+}$ preiPSC to iPSC transition (Fig. 5*A*). Indeed, we found that inducible knockdown of Zfp281 by Dox treatment (shRNA expression is positively marked by RFP, Fig. 5*A, Lower*) resulted in an approximately fourfold increase of both AP(+) (Fig. 5*B, Upper*) and *Oct4*-GFP(+) (Fig. 5*B, Lower*) iPSC colonies. We further confirmed enhanced reprogramming of preiPSCs by Zfp281 down-regulation by using two independent, retrovirally expressed constitutive shRNAs against Zfp281 (Table S1 and Fig. S4 *A* and *B*).

Next, we asked whether the effect of Zfp281 knockdown in promoting the preiPSC to iPSC transition is mediated through endogenous *Nanog* regulation. To this end, we used *Nanog*$^{-/-}$ preiPSCs (8) for the reprogramming assay (Fig. 5*C*). As reported (8), we confirmed that these *Nanog*$^{-/-}$ preiPSCs cannot transit into ground-state, pluripotent iPSCs under 2i+LIF condition unless an exogenous *Nanog* transgene is provided (Fig. 5*D*, black bars). More importantly, we found that knockdown of Zfp281 alone upon Dox induction (+Dox) is no longer effective in promoting the *Nanog*$^{-/-}$ preiPSC to iPSC transition, which is reflected by no colony formation after Dox treatment (Fig. 5*D, Left*, gray bar). These results suggest that the enhanced reprogramming of preiPSCs after Zfp281 down-regulation (Fig. 5*B*) is the direct result of endogenous *Nanog* up-regulation. In addition, although we observed enhanced reprogramming of *Nanog*$^{-/-}$ preiPSCs upon ectopic expression of Nanog (PB-Nanog) in the presence of Dox (i.e., down-regulation of Zfp281), no additive effect of shZfp281 and PB-Nanog relative to PB-Nanog alone was observed (Fig. 5*D, Right*, compare the gray bar with the black

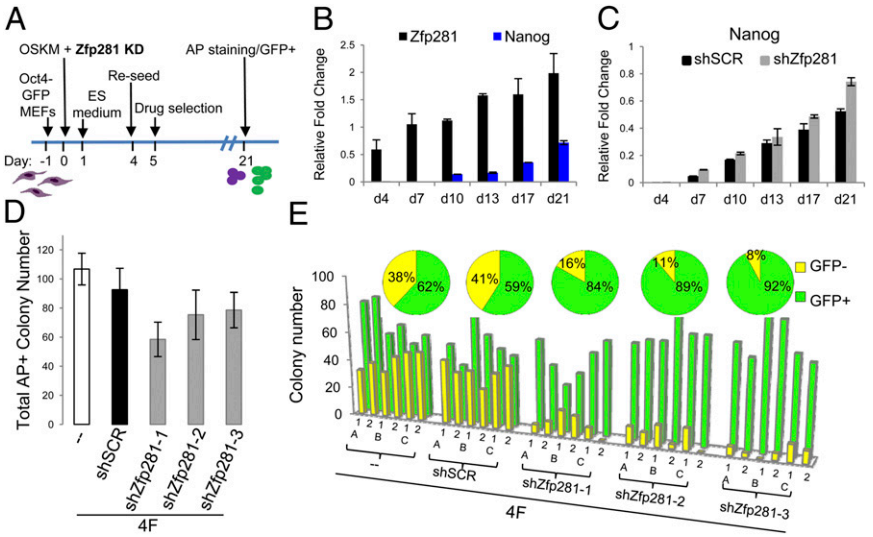

Fig. 4. Loss of Zfp281 facilitates somatic cell reprogramming. (*A*) Summary of the procedure for iPSC generation. (*B*) RT-qPCR analyses of *Zfp281* and *Nanog* expression during iPSC generation. Expression levels were normalized to those in wild-type ESCs. (*C*) RT-qPCR analyses of relative *Nanog* expression during iPSC generation upon knockdown with control scramble (SCR) or Zfp281 shRNA. Expression levels were normalized to those in wild-type ESCs. (*D*) Minimal reduction of total AP (+) colony numbers upon Zfp281 knockdown during reprogramming. (*E*) Zfp281 knockdown promotes iPSC generation. *Oct4*-GFP MEFs were infected with viruses expressing the four reprogramming factors (4F), alone (–) or together with three independent shRNAs against Zfp281 (1–3) and control scramble shRNA (shSCR). The same reprogramming assays were repeated independently three times (A, B, and C) with duplicates each time (1, 2). The average percentages of GFP (+) and GFP (–) colonies from three independent experiments are shown in the pie chart (*Upper*).

bar). These data argue strongly that the regulation of endogenous *Nanog* is the mechanism of Zfp281 action during reprogramming. To further reinforce this conclusion, we performed a similar reprogramming assay by using the *Nanog*$^{+/+}$ preiPSCs in the presence of both Zfp281 knockdown and ectopic *Nanog* expression (Fig. S4*A*). In this case, we observed additive effects of the combined action of *Zfp281* down-regulation (shZfp281) and ectopic Nanog expression (pMx-Nanog) in promoting the *Nanog*$^{+/+}$ preiPSC to iPSC transition (Fig. S4*C*).

Finally, because Nanog overexpressing ESCs can promote reprogramming efficiency when fused with somatic cells (7), we asked whether Nanog up-regulation in *Zfp281*$^{-/-}$ ESCs could also enhance mouse ESC and human B (hB) cell heterokaryon based reprogramming (21) (Fig. S5*A*). Our results show that although reprogramming of hB cells is obvious in both *Zfp281*$^{+/+}$ ESC/hB and *Zfp281*$^{-/-}$ ESC/hB heterokaryons (Fig. S5*C*), an enhanced human ES-specific gene expression profile indicative of improved reprogramming efficiency was observed for *Zfp281*$^{-/-}$ ESC/hB heterokaryons (Fig. S5*B*). These data provide additional validation of the functional implication of Zfp281 in restricting *Nanog* reactivation and impeding reprogramming.

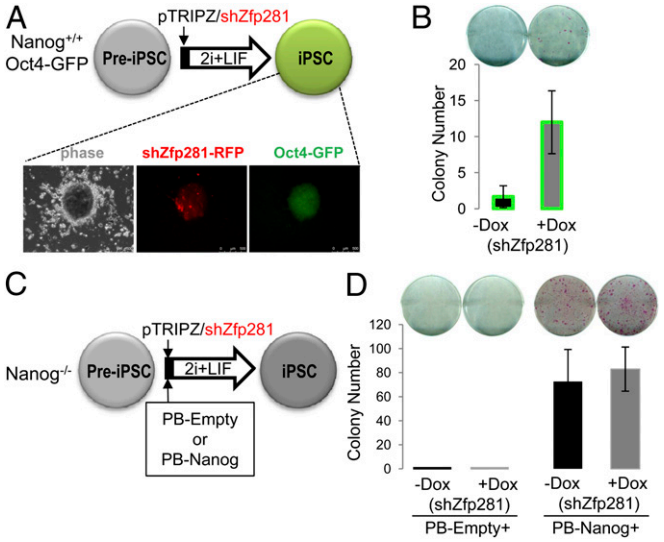

Fig. 5. Zfp281 depletion enhances reprogramming through *Nanog* regulation. (*A*) The strategy for testing the effect of Zfp281 knockdown in the preiPSC to iPSC transition. *Nanog*$^{+/+}$ preiPSCs harboring an *Oct4*-GFP transgene were used for the reprogramming assay as described (19), and iPSCs generated from Zfp281 knockdown are positive for both RFP (for pTRIPZ/shZfp281) and GFP (for *Oct4*-GFP reporter). (*B*) Zfp281 knockdown promotes the *Nanog*$^{+/+}$ preiPSC to iPSC transition. Dox treatment (shZfp281) results in a significant increase of AP (+) (*Upper*) and *Oct4*-GFP (+) (*Lower*) iPSC colony numbers. (*C*) *Nanog*$^{-/-}$ preiPSCs lacking the *Oct4*-GFP transgene (8) were used for the reprogramming assay together with exogenous supply of a *Nanog* transgene in a PiggyBac (PB) vector (PB-Nanog). The empty PB vector (PB-Empty) was used as control. (*D*) Zfp281 knockdown fails to reprogram *Nanog*$^{-/-}$ preiPSCs or augment Nanog-mediated reprogramming of Nanog$^{-/-}$ preiPSCs. A representative image of AP stained colonies (*Upper*) and quantitative data on the total AP (+) colony numbers (*Lower*) are shown. Error bars denote SDs from triplicate wells.

Discussion

In this study, we demonstrate that Nanog is subjected to Zfp281-mediated autoregulation of its own promoter by a negative feedback loop, which we dub Nanog autorepression, and that Zfp281 mediates autorepression by directly recruiting the NuRD repressor complex to the *Nanog* locus and restricts Nanog reactivation during reprogramming. Together with our previous study (16), we have thus established a dual role of Zfp281 for both an important pluripotency factor to fine-tune Nanog expression in maintaining the pluripotent state of ESCs and a transcriptional repressor to restrict *Nanog* activation and impede somatic cell reprogramming. These data offer insights into the regulatory mechanisms underlying optimal ESC state and efficient reprogramming.

Although our results establish Zfp281 as the key transcription regulator mediating Nanog autorepression in ESCs, we note that Zfp281 can directly regulate other pluripotency and developmentally regulated genes as reported (16). Therefore, Nanog derepression is one of many possible regulatory consequences of Zfp281 depletion. Thus, not surprisingly, we found that although down-regulation of Nanog alone in *Zfp281*$^{-/-}$ ESCs rescues the expression of endodermal markers *Gata6* and *Sox17* at a late stage (day 10) of EB differentiation (Fig. S6*C*), it fails to rescue other markers such as *Oct4* and *Cdx2* (Fig. S6*C*) or the EB size/morphology (Fig. S6 *A* and *B*). We also note that Nanog is under negative regulation by other factors including Tcf3 (22). However, the regulatory mechanism is likely different as the binding loci in the *Nanog* regulatory region for Zfp281 (16) and Tcf3 (22) are different and no physical association between the two factors has been detected. In addition, we recognize the importance of positive feedback loops controlled by other stem cell factors such as Oct4-Sox2 heterodimers (23) and Sall4 for Nanog gene activation (14). These observations suggest that Nanog is subjected to multilayered, tight transcriptional

control. Intriguingly, we observed a switch from negative to positive feedback regulation of ^{Endo}*Nanog* by enforced ^{FLbio}*Nanog* expression in the absence of Zfp281 (Fig. 2 *D* and *F*). Because of the concomitant reduction in Nanog binding to its own regulatory regions upon Zfp281 depletion (Fig. 3*B*), we speculate that the activation function of ectopic Nanog observed in *Zfp281*$^{-/-}$ ESCs is more likely resulted from transactivation by other pluripotency factors that act on the endogenous *Nanog* locus. For example, Oct4, Esrrb, and Zfp143 are known to form heterodimers and directly transactivate *Nanog* promoter activity (23–25), and Tbx3 was shown to predominantly stimulate *Nanog* expression in maintaining pluripotency (26). We confirmed Dox-dependent up-regulation of *Oct4*, *Esrrb*, *Zfp143*, *Tbx3*, and *Rex1* in *Zfp281*$^{-/-}$ ESCs but only slightly up-regulated or unchanged levels of these genes in *Zfp281*$^{+/+}$ ESCs (Fig. S7 *A* and *B*), which may partly explain the Nanog activation in *Zfp281*$^{-/-}$ ESCs (Fig. 2*F*).

The Nanog autorepression defined in this study is unique among the core pluripotency network. In fact, down-regulation of other stem cell factor(s) does not lead to the same up-regulation of the corresponding gene promoter activity. For example, down-regulation of Oct4 by siRNA or shRNA leads only to the decrease of *Oct4* promoter activity measured by *Oct4*-GFP reporter expression, which forms the basis for several genome-wide RNAi screening studies for important self-renewal regulators (27–29). Counterintuitively but reassuringly, we found that Nanog siRNA used in a genome-wide RNAi study in NG4 cells resulted in up-regulation of *Nanog*-GFP reporter activity (Fig. S8), consistent with our observation using Nanog shRNA in NG4 cells (Fig. 1 *E* and *F*).

Our study demonstrates that Zfp281 recruits a repressive chromatin remodeling complex, NuRD, to target the *Nanog* promoter/enhancer regions (Figs. 2 and 3). The NuRD complex contains histone deacetylase (HDAC) activity, whose inhibition by valproic acid, an HDAC inhibitor, greatly improves reprogramming efficiency (30). Our biochemical purification and coIP data confirmed association of Zfp281 with NuRD proteins (Fig. 2 *G* and *H*), and ChIP data indicate that binding of NuRD proteins Mta1/2 and Hdac2 to the *Nanog* promoter/enhancer is dramatically reduced upon Zfp281 depletion (Fig. 3 *A*–*C*) and increased upon ectopic Nanog expression (Fig. 3 *D* and *E*). Together with up-regulation of Nanog in Hdac1/2 knockout ESCs (31) and knockdown of NuRD proteins abrogating Nanog autorepression (Fig. 3 *F*–*H*), we provide strong evidence that Zfp281 mediates Nanog autorepression through recruitment of the NuRD repressor complex to the *Nanog* locus. Recent findings have implicated NuRD in choreographing multiple epigenetic events for stem cell pluripotency (see review; ref. 32). However, how NuRD is recruited to the ESC genome remains an open question. It is tempting to ask whether Zfp281 could serve as a sequence-specific transcription factor for global NuRD recruitment to target genes in ESCs. This issue requires delineation of the genomic targets of Zfp281 in ESCs by ChIP-seq.

Understanding how the core pluripotency and reprogramming factors, Nanog and Oct4 in particular, are transcriptionally regulated and function in orchestrating the genetic and epigenetic events that maintain stem cell pluripotency and promote somatic cell reprogramming is subject of intensive studies. We present a detailed mechanistic study demonstrating that Nanog is subjected to a unique transcriptional regulatory mode, i.e., autorepression, which is mediated by one of its transcriptional coregulators, Zfp281 (16). At the molecular level, Nanog autorepression is mediated by Zfp281 and its associated NuRD repressor complex. At the functional level, Nanog autorepression mediated by Zfp281 presents a roadblock to efficient reprogramming.

Methods

ESC Culture and Colony Formation Assays. All mouse ESCs used in this study were grown under standard ESC conditions as described (3). The colony formation assay for ESC self-renewal was performed as described (16).

Nuclear Extract Preparation, Coimmunoprecipitation, Western Blot Analysis, and Affinity Purification of Protein Complexes. All of these procedures have been described in our previous study (2).

Additional Details. The remaining experimental details can be found in *SI Methods*.

ACKNOWLEDGMENTS. This study was supported by National Institutes of Health Grant 1R01-GM095942-01A1, New York State Department of Health Grant NYSTEM#C026420, and a seed fund from the Black Family Stem Cell Institute (to J.W.).

1. Orkin SH, et al. (2008) The transcriptional network controlling pluripotency in ES cells. *Cold Spring Harb Symp Quant Biol* 73:195–202.
2. Ding J, Xu H, Faiola F, Ma'ayan A, Wang J (2012) Oct4 links multiple epigenetic pathways to the pluripotency network. *Cell Res* 22:155–167.
3. Wang J, et al. (2006) A protein interaction network for pluripotency of embryonic stem cells. *Nature* 444:364–368.
4. Wang J (2012) Deciphering protein complexes and protein interaction networks for stem cell pluripotency. *New Frontiers of Network Analysis in Systems Biology*, eds Maayan A, MacArthur BD (Springer Science+Business Media, Dordrecht, The Netherlands), Vol 6, pp 97–118.
5. Kim J, Chu J, Shen X, Wang J, Orkin SH (2008) An extended transcriptional network for pluripotency of embryonic stem cells. *Cell* 132:1049–1061.
6. Chambers I, et al. (2003) Functional expression cloning of Nanog, a pluripotency sustaining factor in embryonic stem cells. *Cell* 113:643–655.
7. Silva J, Chambers I, Pollard S, Smith A (2006) Nanog promotes transfer of pluripotency after cell fusion. *Nature* 441:997–1001.
8. Silva J, et al. (2009) Nanog is the gateway to the pluripotent ground state. *Cell* 138: 722–737.
9. Li JY, et al. (2007) Synergistic function of DNA methyltransferases Dnmt3a and Dnmt3b in the methylation of Oct4 and Nanog. *Mol Cell Biol* 27:8748–8759.
10. Feldman N, et al. (2006) G9a-mediated irreversible epigenetic inactivation of Oct-3/4 during early embryogenesis. *Nat Cell Biol* 8:188–194.
11. Boer B, et al. (2009) Regulation of the Nanog gene by both positive and negative cis-regulatory elements in embryonal carcinoma cells and embryonic stem cells. *Mol Reprod Dev* 76:173–182.
12. Wang J, Orkin SH (2008) A protein roadmap to pluripotency and faithful reprogramming. *Cells Tissues Organs* 188:23–30.
13. Boyer LA, et al. (2005) Core transcriptional regulatory circuitry in human embryonic stem cells. *Cell* 122:947–956.
14. Wu Q, et al. (2006) Sall4 interacts with Nanog and co-occupies Nanog genomic sites in embryonic stem cells. *J Biol Chem* 281:24090–24094.
15. Schaniel C, et al. (2009) Smarcc1/Baf155 couples self-renewal gene repression with changes in chromatin structure in mouse embryonic stem cells. *Stem Cells* 27: 2979–2991.
16. Fidalgo M, et al. (2011) Zfp281 functions as a transcriptional repressor for pluripotency of mouse embryonic stem cells. *Stem Cells* 29:1705–1716.
17. Liang J, et al. (2008) Nanog and Oct4 associate with unique transcriptional repression complexes in embryonic stem cells. *Nat Cell Biol* 10:731–739.
18. Takahashi K, Okita K, Nakagawa M, Yamanaka S (2007) Induction of pluripotent stem cells from fibroblast cultures. *Nat Protoc* 2:3081–3089.
19. Silva J, et al. (2008) Promotion of reprogramming to ground state pluripotency by signal inhibition. *PLoS Biol* 6:e253.
20. Theunissen TW, et al. (2011) Nanog overcomes reprogramming barriers and induces pluripotency in minimal conditions. *Curr Biol* 21:65–71.
21. Pereira CF, Fisher AG (2009) Heterokaryon-based reprogramming for pluripotency. *Curr Protoc Stem Cell Biol*, Chapter 4:Unit 4B.1.
22. Yi F, Pereira L, Merrill BJ (2008) Tcf3 functions as a steady-state limiter of transcriptional programs of mouse embryonic stem cell self-renewal. *Stem Cells* 26: 1951–1960.
23. Rodda DJ, et al. (2005) Transcriptional regulation of nanog by OCT4 and SOX2. *J Biol Chem* 280:24731–24737.
24. van den Berg DL, et al. (2008) Estrogen-related receptor beta interacts with Oct4 to positively regulate Nanog gene expression. *Mol Cell Biol* 28:5986–5995.
25. Chen X, Fang F, Liou YC, Ng HH (2008) Zfp143 regulates Nanog through modulation of Oct4 binding. *Stem Cells* 26:2759–2767.
26. Niwa H, Ogawa K, Shimosato D, Adachi K (2009) A parallel circuit of LIF signalling pathways maintains pluripotency of mouse ES cells. *Nature* 460:118–122.
27. Chia NY, et al. (2010) A genome-wide RNAi screen reveals determinants of human embryonic stem cell identity. *Nature* 468:316–320.
28. Ding L, et al. (2009) A genome-scale RNAi screen for Oct4 modulators defines a role of the Paf1 complex for embryonic stem cell identity. *Cell Stem Cell* 4:403–415.
29. Hu G, et al. (2009) A genome-wide RNAi screen identifies a new transcriptional module required for self-renewal. *Genes Dev* 23:837–848.
30. Huangfu D, et al. (2008) Induction of pluripotent stem cells by defined factors is greatly improved by small-molecule compounds. *Nat Biotechnol* 26:795–797.
31. Dovey OM, Foster CT, Cowley SM (2010) Histone deacetylase 1 (HDAC1), but not HDAC2, controls embryonic stem cell differentiation. *Proc Natl Acad Sci USA* 107:8242–8247.
32. Hu G, Wade P (2012) NuRD and pluripotency: A complex balancing act. *Cell Stem Cell* 10:497–503.

Supporting Information

Fidalgo et al. 10.1073/pnas.1208533109

SI Methods

Generation of Transgenic NG4 ESC Lines. NG4 ESCs have been described (1). For ectopic Nanog expression, a Flag and biotin-tagged doxycycline-inducible Nanog transgene (^{FLbio}*Nanog*) was introduced into NG4 cells by lentiviral infection using a pTRIPZ vector. Positive clones were established by puromycin (1 μg/mL) selection, and expression of ^{FLbio}*Nanog* upon Doxycycline (Dox) treatment (0, 0.625, 1.25, or 2.5 μg/mL) was confirmed by RT-quantitative PCR (qPCR). The same Dox concentrations were used throughout the study. For knockdown studies, ESCs were infected with pLKO lentiviruses expressing no shRNA (shEmpty) or shRNA against Nanog (shNanog) or NuRD complex proteins followed by selection with puromycin (1 μg/mL) for 48 h. The pLKO.1 lentiviral vector contains a puromycin-IRES-mCherry "pim" expression cassette.

In Vitro Differentiation. Differentiation of ESCs to embryoid bodies (EBs) was performed as described in our previous study (2). Briefly, shRNA virus transduced ESCs described above were cultured in suspension on low attachment dishes in standard ES medium over a 10-d period in the absence of LIF and in the presence of puromycin. The area of EBs was calculated by using ImageJ software.

Validation of Anti-Zfp281 Antibody for Immunoprecipitation, Coimmunoprecipitation (Co-IP), and Western Blot Analyses. We have used an anti-Zfp281 antibody for both IP/co-IP and affinity purification. The quality of this antibody has been validated (Fig. S2 *A* and *B*). This antibody is commercially available from Abcam (ab101318). Other commercially available antibodies used in this study are as follows: anti-Nanog (AB5731, Millipore; A300-397A, Bethyl), anti-Chd4 (A301-081A, Bethyl), anti-Mta1/2 (A300-911A, Bethyl), anti-HDAC2 (A300-705A, Bethyl), and anti-β-Actin (A5441, Sigma).

Generation of iPSCs from *Oct4*-GFP Mouse Embryonic Fibroblasts (MEFs). For lentivirus production, STEMCCA plasmid (3) was cotransfected with packaging vectors into HEK293T cells. For retroviral production Plat-E cells were transfected with an LMP-shRNA scramble vector and LMP-shRNA against Zfp281. The viral supernatants were harvested after 48 h and concentrated by using Amicon Ultra (Millipore) centrifuge tubes. Reprogramming was performed according to a published procedure (3) with minor changes. Briefly, STEMCCA lentiviral supernatants containing the four reprogramming factors (Oct4, Sox2, Klf4, and cMyc; OSKM) and retroviral LMP-shRNA supernatants were mixed before infection. Infected cells were selected with puromycin (1.5 μg/mL) at day five after transduction, and selection was maintained for 15 d. iPSC colonies were scored 21 d after transduction by counting GFP-positive colonies under fluorescence microscope or by staining for alkaline phosphatase (AP) activity using a commercial kit (Sigma). Quantitation of GFP(+) cells during reprogramming was also performed by flow cytometry analysis.

Generation of iPSCs from Neural Stem (NS) Cell Reprogrammed PreiPSCs. *Nanog*$^{+/+}$ or *Nanog*$^{-/-}$ NS cells were reprogrammed to preiPSCs by Oct4, Klf4, and c-Myc (4, 5). These preiPSCs were infected with lentiviruses (pTRIPZ) or retroviruses (LMP or pMx) expressing shZfp281 (V2THS_42594, Open Biosystems; Table S1), scramble shRNA (shSCR), or Nanog cDNA (PiggyBac or PB-Nanog, pMx-Nanog), followed by selection with puromycin (2 μg/mL) for at least 10 d. Transduced preiPSC cells (1×10^5) were seeded on a six-well plate in serum/LIF medium. After 4 d, medium was switched to serum-free N2B27 supplemented medium with LIF and 2i inhibitors, CHIR99021 (3 μM; STEMGENT) and PD025901 (1 μM; STEMGENT). *Oct4*-GFP positive colonies from reprogrammed *Nanog*$^{+/+}$ preiPSCs or AP positively stained colonies from both *Nanog*$^{+/+}$ and *Nanog*$^{-/-}$ preiPSCs were scored at day 10 after 2i/LIF treatment.

Heterokaryon-Based Reprogramming. Experimental heterokaryons were generated by fusing mouse ESCs and human B lymphocytes according to a published protocol (6). *Zfp281*$^{+/+}$ and *Zfp281*$^{-/-}$ ESCs (2) were used for fusion with human B cells as described (6). Reprogramming of human somatic cells was monitored by quantitative real-time PCR analyses of human-specific gene expression. The sequences of human gene-specific primers are provided in Table S1.

Flow Cytometry. For flow cytometry analyses, single-cell suspensions were evaluated on an LSRII Flow Cytometer System (BD Biosciences). Data were analyzed with FlowJo software.

Chromatin Immunoprecipitation Coupled with Quantitative Real-Time PCR (ChIP-qPCR). ChIP assays were performed as described (7). Briefly, cells were cross-linked with 1% (wt/vol) formaldehyde for 5 min at room temperature, and formaldehyde was inactivated by the addition of 125 mM glycine. Chromatin extracts containing DNA fragments were immunoprecipitated by using anti-Nanog (Bethyl), anti-Zfp281 (Fig. S2), anti-Mta1/2 (Bethyl), or anti-HDAC2 (Bethyl) antibodies. Immunoprecipitated DNA was analyzed by real-time PCR as described (2), and the primer sequences are provided in Table S1. Measurements were performed in triplicate, and error bars denote SDs.

1. Schaniel C, et al. (2009) Smarcc1/Baf155 couples self-renewal gene repression with changes in chromatin structure in mouse embryonic stem cells. *Stem Cells* 27: 2979–2991.
2. Fidalgo M, et al. (2011) Zfp281 functions as a transcriptional repressor for pluripotency of mouse embryonic stem cells. *Stem Cells* 29:1705–1716.
3. Sommer CA, et al. (2009) Induced pluripotent stem cell generation using a single lentiviral stem cell cassette. *Stem Cells* 27:543–549.
4. Silva J, et al. (2008) Promotion of reprogramming to ground state pluripotency by signal inhibition. *PLoS Biol* 6:e253.
5. Silva J, et al. (2009) Nanog is the gateway to the pluripotent ground state. *Cell* 138: 722–737.
6. Pereira CF, Fisher AG (2009) Heterokaryon-based reprogramming for pluripotency. *Curr Protoc Stem Cell Biol*, Chapter 4:Unit 4B.1.
7. Lee TI, Johnstone SE, Young RA (2006) Chromatin immunoprecipitation and microarray-based analysis of protein location. *Nat Protoc* 1:729–748.

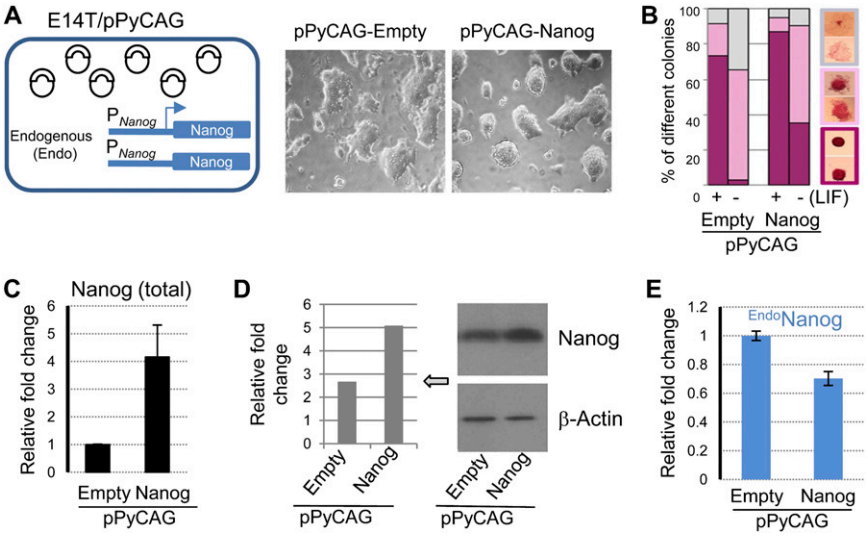

Fig. S1. Nanog autorepression in E14T cells. (*A*) Schematic representation of an episomal system for enforced *Nanog* expression in E14T ESCs (*Left*) and morphology of established E14T cell lines expressing empty vector or pPyCAG-Nanog (*Center* and *Right*). (*B*) Colony formation assays show that enforced *Nanog* expression sustains LIF-independent self-renewal. Colonies stained for AP were scored in three categories: uniformly undifferentiated (purple), partially differentiated (pink), and fully differentiated (gray) as indicated on the right. (*C*) Total *Nanog* transcripts analyzed by reverse transcription-quantitative PCR (RT-qPCR). Error bars represent SD (n = 3). (*D*) Total Nanog protein expression by Western blotting. Quantitation of protein expression was performed with ImageJ software, and results are presented on *Left*. β-Actin was used as a loading control. (*E*) RT-qPCR analyses of endogenous *Nanog* (^{Endo}*Nanog*) transcripts. Error bars represent SD (n = 3).

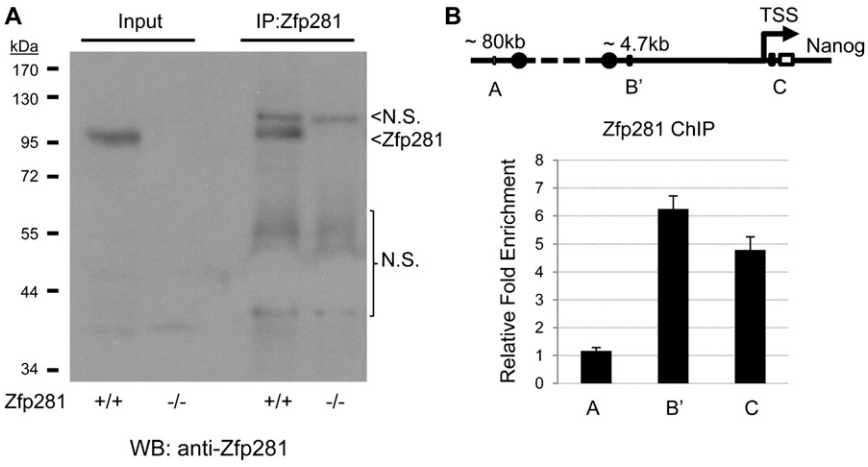

Fig. S2. Validation of Zfp281 antibody. (*A*) The Zfp281 antibody is specific for both Western blot and immunoprecipitation (IP) detection of Zfp281 protein. Zfp281 is detected by Western blot after IP of nuclear extracts from *Zfp281*$^{+/+}$ ESCs. Note that the specific band detected by Western blot disappears in the nuclear extracts from *Zfp281*$^{-/-}$ ESCs, confirming the specificity of the antibody. N.S., nonspecific signals enriched in both *Zfp281*$^{+/+}$ and *Zfp281*$^{-/-}$ ESCs during IP. (*B*) Relative enrichment of Zfp281 in the genomic loci of *Nanog* using chromatin from *Zfp281*$^{+/+}$ ESCs. Illustration of the upstream regulatory regions of the *Nanog* gene is shown (*Upper*), and primers are listed in Table S1.

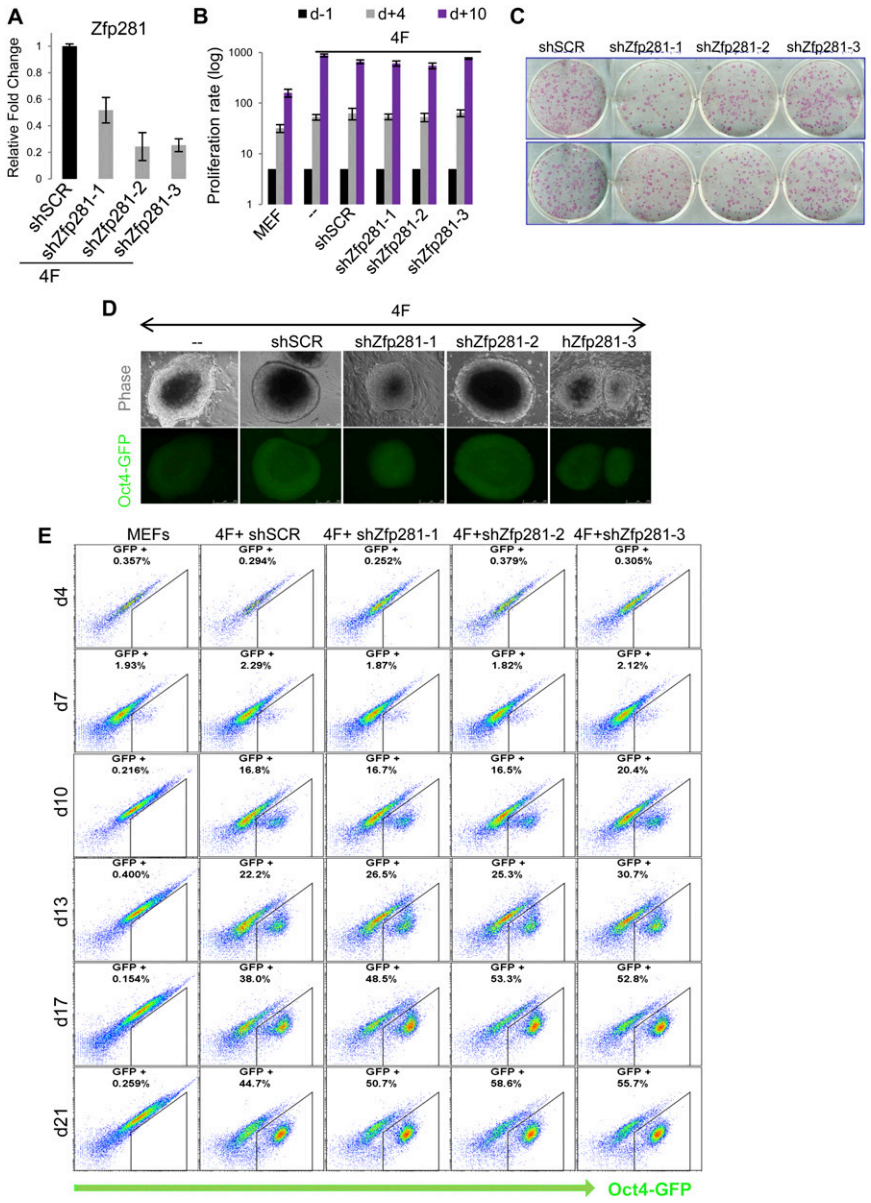

Fig. S3. Down-regulation of Zfp281 enhances the efficiency of somatic cell reprogramming. (*A*) RT-qPCR analyses of *Zfp281* expression after knockdown with three independent shRNAs targeting Zfp281. MEFs were transduced with STEMCCA lentivirus expressing four reprogramming factors (4F) (Oct4, Sox2, Klf4, and c-Myc) and LMP virus expressing a scrambled shRNA sequence (shSCR) or three independent shRNAs against Zfp281 and grown for 4 d. The data were normalized to *Gapdh*, and error bars represent the SD of triplicate qPCR reactions. (*B*) Mean proliferation rate of MEFs. Cells were counted at each time point as indicated. (*C*) iPSC colonies were stained for AP activity 21 d after transduction. Duplicated wells from the same experiment are shown. (*D*) Phase and GFP images of iPSC colonies 21 d after transduction. (*E*) Flow cytometry analysis of *Oct4*-GFP cells during iPSC reprogramming at indicated days after virus infection.

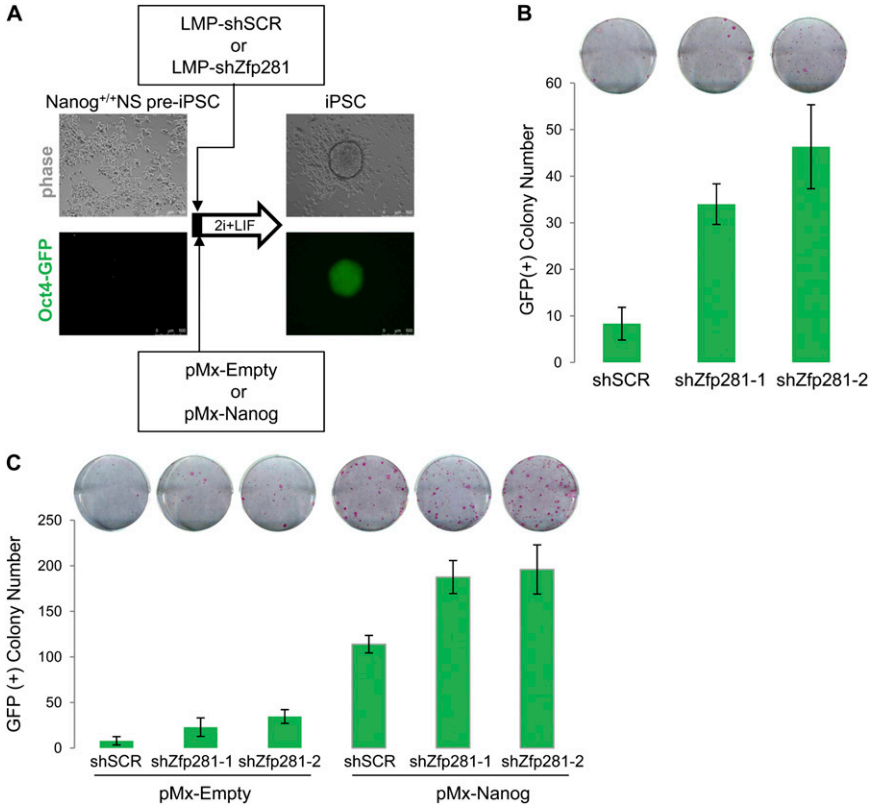

Fig. S4. Loss of Zfp281 facilitates somatic cell reprogramming through *Nanog* regulation. (*A*) Summary of the procedure for iPSC generation using *Nanog*$^{+/+}$ preiPSCs. These preiPSCs harbor an *Oct4*-GFP transgene that can be reactivated during reprogramming. (*B*) Zfp281 knockdown promotes the preiPSC to iPSC transition. (*B Upper*) AP positive colonies in representative wells. (*B Lower*) GFP (+) colony numbers. (*C*) Enhanced reprogramming by combined action of Zfp281 knockdown (shZfp281) and ectopic Nanog expression (pMx-Nanog) in *Nanog*$^{+/+}$ preiPSCs. *Nanog*$^{+/+}$ preiPSCs were infected with indicated shRNAs in combination with retroviral pMx-Nanog or pMx vector alone. (*C Upper*) AP positive colonies in representative wells. (*C Lower*) GFP (+) colony numbers.

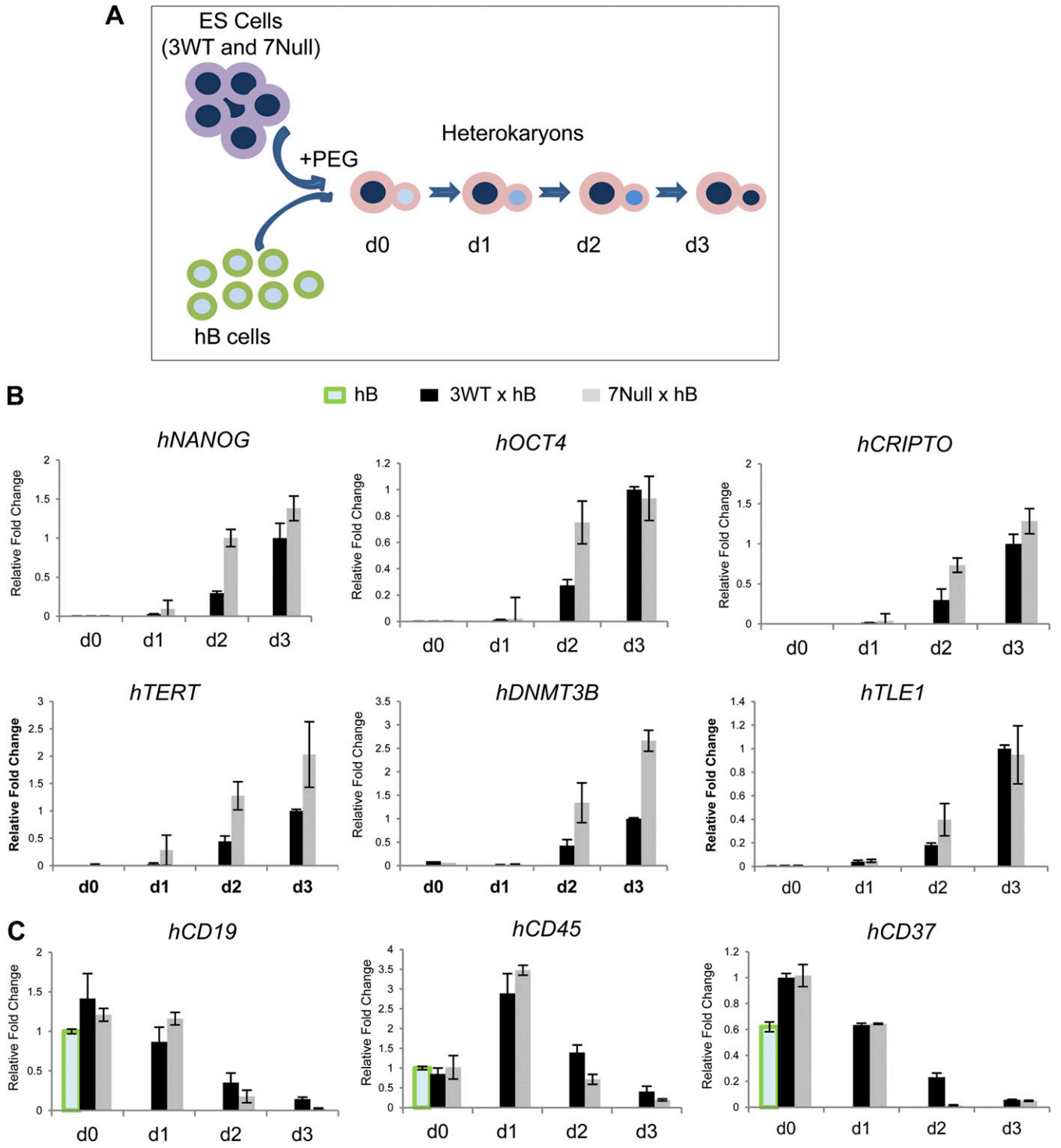

Fig. S5. Loss of Zfp281 enhances heterokaryon-based reprogramming. (*A*) Schematic representation of the strategy for generating heterokaryons between mouse ESCs and human B lymphocytes. *Zfp281*$^{+/+}$ (3WT) and *Zfp281*$^{-/-}$ (7Null) ESCs have been described (2) and were used as fusion partners for human B (hB) cells. (*B*) Enhanced reprogramming of human pluripotency gene expression in hB cells by *Zfp281*$^{-/-}$ ESCs. (*C*) Down-regulation of hB cell-specific genes during reprogramming.

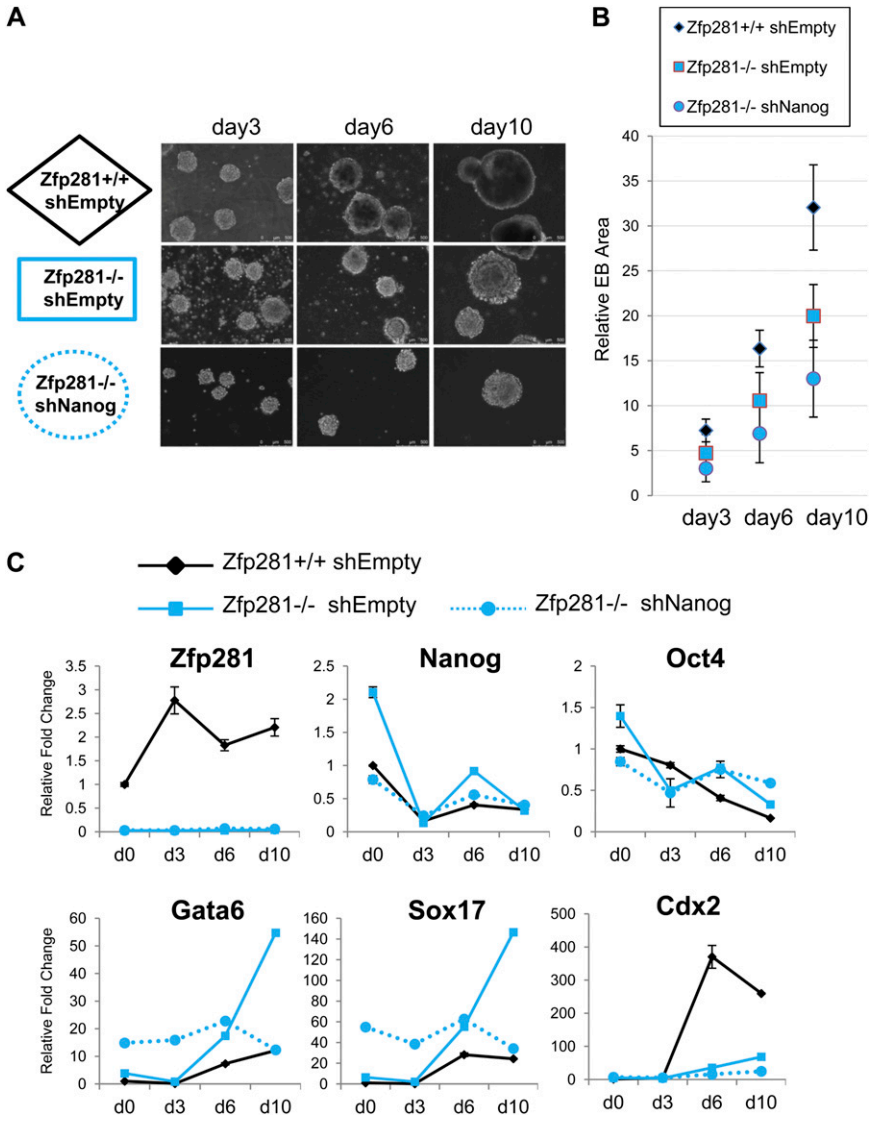

Fig. S6. Down-regulation of Nanog fails to rescue differentiation defects of *Zfp281*$^{-/-}$ ESCs during in vitro differentiation. (*A*) Representative images of EBs generated from ESCs transduced with shEmpty or shNanog in the presence or absence of Zfp281. (*B*) Analysis of the relative EB area during the time course of EB differentiation. Note that down-regulation of Nanog fails to rescue the smaller EB phenotype of *Zfp281*$^{-/-}$ ESCs. (*C*) RT-qPCR analyses of relative expression levels of *Nanog*, *Oct4*, *Gata6*, *Sox17*, and *Cdx2* during the time course of EB differentiation.

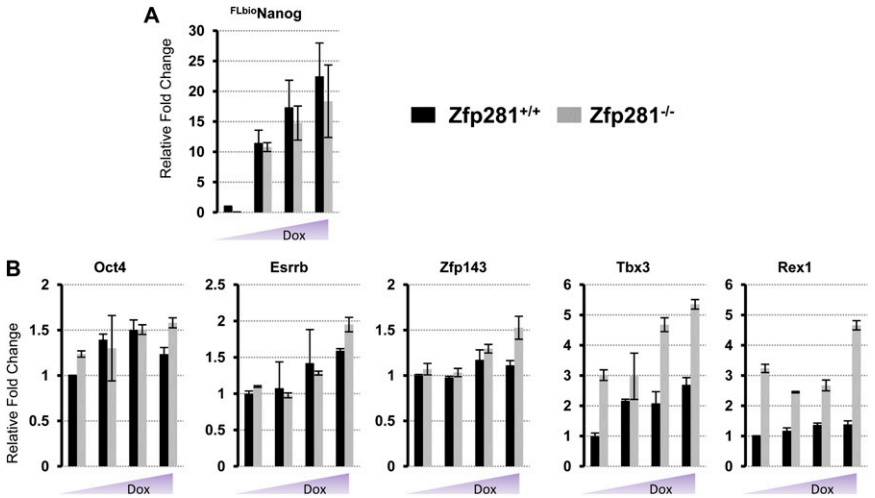

Fig. S7. Ectopic expression of Nanog promotes activation of known *Nanog* activators in the absence of Zfp281. (*A*) RT-qPCR analyses of ectopic *Nanog* (*^{FLbio}Nanog*) expression upon Dox treatment in *Zfp281$^{+/+}$* and *Zfp281$^{-/-}$* ESCs. (*B*) RT-qPCR analyses of *Oct4*, *Esrrb*, *Zfp143*, *Tbx3,* and *Rex1* expression in the same samples as described in *A*.

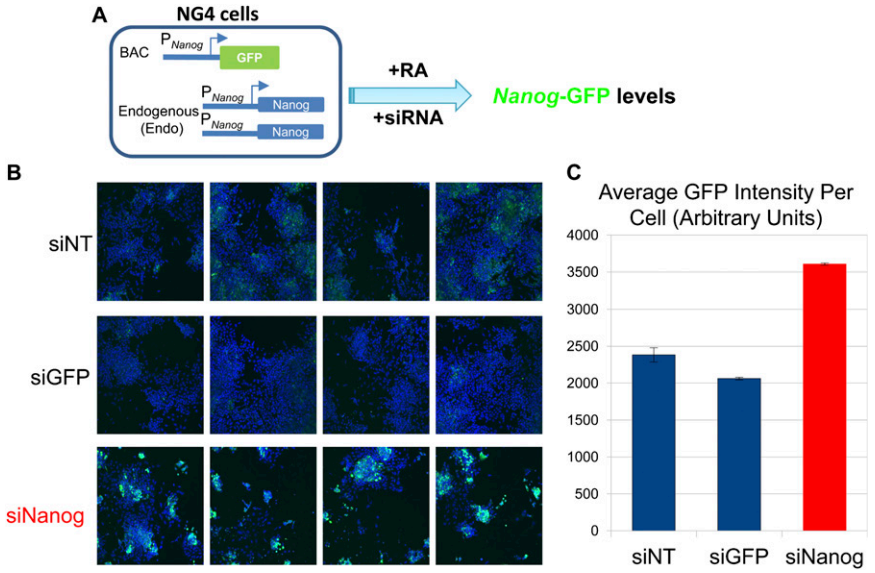

Fig. S8. Down-regulation of Nanog by siRNA causes up-regulation of *Nanog*-GFP reporter activity. (*A*) Schematic depiction of the genome-wide siRNA screening strategy. NG4 cells were reverse-transfected with 25 nM siRNA in 384-well tissue culture plates coated with 0.1% gelatin in 50 μL of total volume with standard mouse ES media containing LIF. After 1 d, media were changed to ES media without LIF plus 10 nM RA for 2 d. Cells were fixed with 2% formaledhyde in PBS for 15 min and stained with Hoechst 33342 (5 μg/mL) before confocal fluorescence imaging. (*B*) Representative high-content images of NG4 cells treated with nontargeting siRNA control (siNT), siRNA against GFP (siGFP), and siRNA against Nanog (siNanog). (*C*) Quantitation of average GFP intensity per cell. Note the increase of GFP intensity upon siNanog treatment.

Table S1. List of qPCR primers, ChIP-qPCR primers, and shRNA oligos used in this study

Primer name	Primer sequence
qPCR analysis	
Nanog F (End)	TTGCTCTTTCTGTGGGAAGG
Nanog R (end)	CCAGGAAGACCCACACTCAT
Nanog F (total)	AGGGTCTGCTACTGAGATGCTCTG
Nanog R (total)	CAACCACTGGTTTTTCTGCCACCG
Nanog F (Flagbio)	GCAAGAAGAGCATCTGTGGA
Nanog R (Flagbio)	AAAACTGCAGGCATTGATGA
Gapdh F	ACCCAGAAGACTGTGGATGG
Gapdh R	CACATTGGGGGTAGGAACAC
Gatad2b F	CCCAGCAGATGAGCGAGAT
Gatad2b R	TCTTCATAACCCTTGACACCACT
Mta2 F	TCGGGAGTTTGAGGAGGAATC
Mta2 R	CCCTTATGTGGGTGGCTGGTA
Mta3 F	CCACTTACGGATCGACAGATTG
Mta3 R	GGCGCTGCTGAGGTCATAG
Cdx2 F	CAAGGACGTGAGCATGTATCC
Cdx2 R	GTAACCACCGTAGTCCGGGTA
Esrrb F	CAGGCAAGGATGACAGACG
Esrrb R	GAGACAGCACGAAGGACTGC
Gata6 F	TTGCTCCGGTAACAGCAGTG
Gata6 R	GTGGTCGCTTGTGTAGAAGGA
Oct4 F	CTGAGGGCCAGGCAGGAGCACGAG
Oct4 R	CTGTAGGGAGGGCTTCGGGCACTT
Rex1 F	CAGTCCAGAATACCAGAGTGGAA
Rex1 R	ACTCTAGGTATCCGTCAGGGAAG
Sox17 F	CGCACGGAATTCGAACAGTA
Sox17 R	GTCAAATGTCGGGGTAGTTG
Tbx3 F	TTATTTCCAGGTCAGGAGATGGC
Tbx3 R	GGTCGTTTGAACCAAGTCCCTC
Zfp143 F	CAGGTCAAGGTGATGATGTTCTTAAAGGGT
Zfp143 R	GGCCTGCATGTCAGCTTGAGATATG
Zfp281 F	ACCTGGTGGCAGAGCTTGTGT
Zfp281 R	AGAGCAGAGCCACTGCCTATC
CD19 F (human)	GCTCAAGACGCTGGAAAGTATTATT
CD19 R (human)	GATAAGCCAAAGTCACAGCTGAGA
CD37 F (human)	GTGGCTGCACAACAACCTTATTT
CD37 R (human)	GCCTAACGGTATCGAGCGAG
CD45 F (human)	CCCCATGAACGTTACCATTTG
CD45 R (human)	GATAGTCTCCATTGTGAAAATAGGCC
CRIPTO F (human)	AGAAGTGTTCCCTGTGTAAATGCTG
CRIPTO R (human)	CACGAGGTGCTCATCCATCA
DNMT3b F (human)	GTCAAGCTACACACAGGACTTGACAG
DNMT3b R (human)	AGTTCGGACAGCTGGGCTTT
GAPDH F (human)	TCTGCTCCTCCTGTTCGACA
GAPDH R (human)	AAAAGCAGCCCTGGTGACC
NANOG F (human)	CCAACATCCTGAACCTCAGCTAC
NANOG R (human)	GCCTTCTGCGTCACACCATT
OCT4 F (human)	TCGAGAACCGAGTGAGAGGC
OCT4 R (human)	CACACTCGGACCACATCCTTC
TERT F (human)	GCCAGCATCATCAAACCCC
TERT R (human)	CTGTCAAGGTAGAGACGTGGCTC
TLE1 F (human)	TGTCTCCCAGCTCGACTGTCT
TLE1 R (human)	AAGTACTGGCTTCCCCTCCC
ChIP-qPCR analysis	
Gapdh F	AAGCTCATGAGGCACAGAATGGTC
Gapdh R	TGGGTACATGGTGACTTTCCTAGGC
Nanog-A F	GGCATTTGTGAGTATAGGGGTAGG
Nanog-A R	CCTGTTCTGTGTCAGCACACTTAG
Nanog-B′ F	GTTTTGACTGCTAACCACCCAGAG
Nanog-B′ R	GGCAGGCTTGCTACATTCCTTATC
Nanog-B′′ F	ACTCCAAGGCTAGCGATTCA
Nanog-B′′ R	AATAGGGAGGAGGGCGTCTA

Table S1. Cont.

Primer name	Primer sequence
Nanog-C F	AATGAGGTAAAGCCTCTTTTTGG
Nanog-C R	ACCATGGACATTGTAATGCAAA
shRNA sequences	
shChd4	CCTGAGAGGTTCCACAACTTA
shGatad2b	TCAACGTGTTATTGCACCAAA
shLuciferase (shLuci)	CTTACGCTGAGTACTTCGA
shMta2	CGGGAAGGATTTCAATGATAT
shMta3	CGGCAAAGATTTCAACGACAT
shNanog	GACAGTGAGGTGCATATAC
shZfp281-1	GTCATCAAACCATAACAGTA
shZfp281-2	GCCCGATAAGTAGTAATTA
shZfp281-3	CTCTAAATGCTGAAATTAAG
shZfp281 (pTRIPZ-shRNAmir)	V2THS_42594 (Open Biosystems)

F, forward primer; R, reverse primer.